Journal of Applied Polymer Science

Functionalized KIT-6/Terpolyimide Composites with Ultra-Low Dielectric Constant

Revathi Purushothaman,[1] Muthiapillai Palanichamy,[2] I. Mohammed Bilal[1]
[1]Department of Chemistry, B.S. Abdur Rahman University, Vandalur, Chennai 600048
[2]Department of Chemistry, Anna University, Chennai 600025, India
Correspondence to: R. Purushothaman (E-mail: purushothrevathi@gmail.com)

ABSTRACT: Polyimides with low dielectric constants are important raw materials for the fabrication of flexible printed circuit boards and other microelectronic applications. As creation of voids in polyimide matrix could decrease dielectric constant, in this study mesoporous KIT-6, synthesized hydrothermally, was functionalized with 3-aminopropyltriethoxysilane (APTS) and mixed with 4,4′-oxydianiline (ODA) in the synthesis of terpoly(amic acid) using 3,3′,4,4′-biphenyldianhydride (BPDA), 3,3′,4,4′-oxydiphthalic dianhydride (ODPA) and 3,3′,4,4′-benzophenonetetracarboxylic dianhydride (BTDA) and subsequently stage-cured to obtain APTS-KIT-6/Terpolyimide composites (APTS-KIT-6/TPI). The asymmetric and symmetric vibrations of imide O═C—N—C═O groups of APTS-KIT-6/TPI composites showed their peaks at 1772 and 1713 cm^{-1}. The dielectric constant decreased with the increase in KIT-6 loading from 2 to 4%, but increased at higher loadings, and at 4% loading it was 1.42. Its tensile strength (103 MPa), tensile modulus (2.5 GPa), and percentage elongation (8.2) and high thermal stability (>540°C) were also adequate for application in microelectronics such as flexible printed circuits. © 2014 Wiley Periodicals, Inc. J. Appl. Polym. Sci. **2014**, *131*, 40508.

KEYWORDS: dielectric properties; composites; films; porous materials; polyimides

Received 4 November 2013; accepted 25 January 2014
DOI: 10.1002/app.40508

INTRODUCTION

Polyimides are well known for their high temperature stability, good mechanical properties, excellent chemical stability, low thermal expansion coefficients, and low dielectric constants.[1–3] They have been widely used as interdielectric materials in microelectronics and large scale IC industry, as electrical insulations for conventional appliances, and as functional materials for other industrial applications. Though a number of investigations have been undertaken to synthesize polyimides and copolyimides with excellent thermal, mechanical, and chemical properties, their dielectric constants lie between 3 and 4. Hence in recent years the preparation of polyimides with still low dielectric constants and high performance has become one of the major research challenges for applications in microelectronics. Several approaches were made to reduce the dielectric constants of polyimides which include (i) incorporation of fluorinated substituents into polyimide back bones[4–6] (ii) thermal degradation of the labile block or graft chains in the copolyimides,[7,8] and (iii) introduction of air gaps into interconnected structures and nanopores into polymers.[9–11] Considering that incorporation of air (dielectric constant = 1) can reduce the dielectric constant remarkably by resulting in porous structure, most studies were focused on the last two approaches. Lin and Wang[10] and Min et al.[11] synthesized novel mesoporous silica/polyimide composites using SBA-15 and SBA-16 but their dielectric constants were between 2.6 and 2.73. Some of the organosoluble fluorinated polyimides were synthesized with dielectric constant between 2.75 and 3.24.[12,13] The literature survey reveals that much work has been focused on the synthesis of homo and copolyimides for lowering dielectric constant but not on terpolyimides. There is an advantage in selecting terpolyimides, as properties like mechanical, thermal, and dielectric constant could be tailor-made in them by changing the compositions of the monomers. The mechanical and thermal properties of the terpolyimides derived from different compositions of BPDA, BTDA, ODPA, and ODA were enhanced, but their dielectric constants were in the range of 3.52–5.82.[14,15]

To further reduce dielectric constant of such terpolyimides, in this study it was planned to exploit the use of mesoporous material such as KIT-6, as it could create mesoporous voids. The free uncondensed Si—OH groups (defective Si—OH groups) present in KIT-6 should be completely masked, as they might increase dielectric constant. To improve the compatibility of KIT-6 with terpolyimides and to mask the defective Si—OH groups present, it was functionalized with 3-aminopropyltriethoxysilane (APTS). APTS-KIT-6/TPI composite films were prepared with different

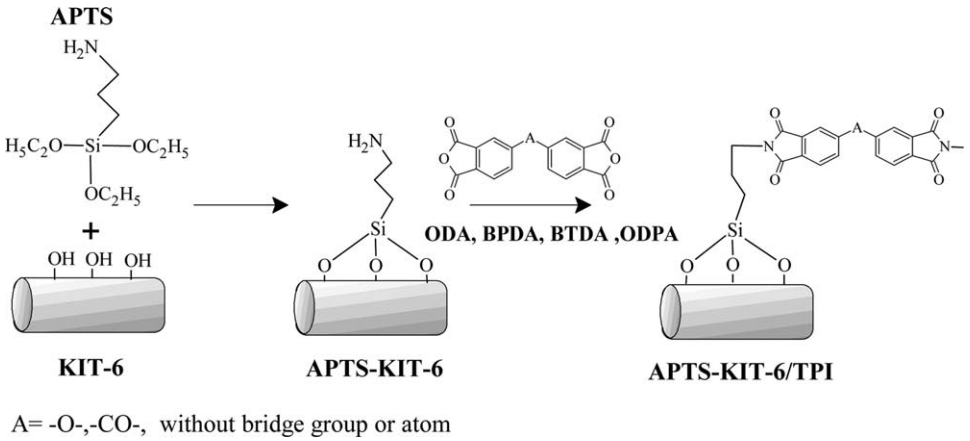

Scheme I. Synthesis of APTS-KIT-6/Terpolyimide composite.

loadings of APTS-KIT-6 and also investigated its effect on mechanical, thermal, and dielectric properties.

EXPERIMENTAL

Materials

4,4′-Oxydianiline (ODA) (Alfa Aesar, m.p.−191.5–193°C), 3,3′,4,4′-biphenyldianhydride (BPDA) (Sigma Aldrich, m.p.−299–305°C), 3,3′,4,4′-oxydiphthalicdianhydride (ODPA) (Sigma Aldrich, m.p.−225–229.4°C) and 3,3′,4′-benzophenonetetracaboxylicdianhydride (BTDA) (Alfa Aesar, m.p.−219–226°C) were used as-received after drying. 3-Aminopropyltriethoxysilane (APTS) (Alfa Aesar), methanol (Merck), 37.5 wt % hydrochloric Acid (Merck), n-butanol (Merck) and anhydrous *N,N*-dimethylacetamide (DMAc) (Aldrich) were used as-received.

Synthesis 3of KIT-6 and APTS Functionalization

KIT-6, large-pore cubic Ia3d mesoporous silica, was synthesized using the tri-block copolymer, EO20-PO70-EO20, and n-butanol as a structure-directing mixture. In a typical synthesis, 4.0 g of P123 was dissolved in 144 g of distilled water and 6.5 mL of 35 wt % HCl in a 500 mL round-bottomed flask under stirring at 35°C for 3 h. Totally, 4.0 g of n-butanol was then added. After 2 h stirring, 8.6 g of TEOS was added to the homogeneous solution drop wise for 4 h with a pressure equalizing funnel. This mixture was kept under vigorous stirring at 35°C for 24 h. Subsequently, the mixture was aged at 100°C for 24 h in a hot air oven. The product was hot filtered without washing and dried at 100°C for 24 h in air. Surfactant-free KIT-6 was obtained after a brief ethanol/HCl washing and subsequent calcination at 550°C in air.[16]

3-Aminopropyl triethoxy silane (APTS) was covalently bonded to calcined KIT-6 by the reaction of it with the defective Si—OH groups of the latter. 2.5 g of mesoporous silica was dispersed in 60.2 mL of ethanol under ultrasonic agitation for 1 h, and 0.625 g of APTS was added to the mixture, stirred for 24 h with a magnetic stirrer at 30°C. Then the mixture was filtered and the solid product washed several times using ethanol and dried in a vacuum oven at room temperature to obtain APTS functionalized KIT-6 (APTS-KIT-6).

Synthesis of APTS-KIT-6/Terpolyimide Composites

APTS-KIT-6/TPI composite films were prepared via a two-step pathway with different loadings of APTS-KIT-6 (2, 4, 6, 8, and 10 wt %). In the first step, a calculated amount of APTS-KIT-6 in DMAc was added to a three-necked round bottomed flask and subjected to ultrasonic agitation for 1 h. ODA was added to it and the mixture magnetically stirred. After dissolving ODA completely, a solid mixture of BPDA, BTDA and ODPA with a mole ratio of (0.5 : 0.25 : 0.25) was added in one lot with additional DMAc so as to adjust the solid content to 40% (weight to volume). The reaction mixture was stirred for 24 h in the nitrogen atmosphere at ambient temperature until a viscous solution was obtained. The resulting PAA solution of 0.65 mm thickness was doctored onto a clean dry glass plate using a solution casting machine and stage-cured in a vacuum oven up to 300°C for 13 h. Finally, the film was peeled off from the glass plate (Scheme I). Terpolyimide film (TPI) was also prepared without APTS-KIT-6 for comparison (Scheme 2).

Measurements

Fourier transform infrared (FTIR) spectra of as-synthesized KIT-6, calcined KIT-6, APTS-KIT-6 samples (KBr), and APTS-KIT-6/Terpolyimide composite films were obtained with a Perkin-Elmer Spectrum 100 Fourier transform spectrometer. The Thermogravimetric analyses of as-synthesized, calcined and APTS-KIT-6 samples were analyzed using SCINCO N-1000 at a heating rate of 10°C/min in a nitrogen atmosphere from ambient to 700°C. Thermogravimetric analyses (TGA) and Differential Scanning Calorimetry (DSC) of finely chopped APTS-KIT-6/TPI composite films (~10 mg) was carried out between ambient and 1000°C on a Mettler TGA-DSC 1 model thermal analyzer at a heating rate of 10°C/min with the film sample sealed in an alumina pan. Dynamic mechanical analysis (DMA) was utilized to determine storage and loss moduli as well as tanδ of APTS-KIT-6/TPI composite films. The analysis was undertaken in a SEIKO EXSTAR DMS 6100. For 30–40 μm thermally cured films, the tension-mode deformation was used at a frequency of 1 Hz and a heating rate of 3°C/min under nitrogen. Powder X-ray diffraction patterns (XRD) were recorded using a Rigaku Miniflex diffractometer with Cu-Kα radiation ($\lambda = 0.154$ nm). The diffraction data were recorded over the 2θ range 0.5–10° at a 0.02° step size with 1 s step time for samples of calcined and APTS-KIT-6. The nitrogen adsorption-desorption isotherms were measured at -196°C on a BELCAT nitrogen-desorption analyzer. Prior to each adsorption measurement, the samples were evacuated at 100°C under vacuum ($P < 10^{-5}$ torr) through

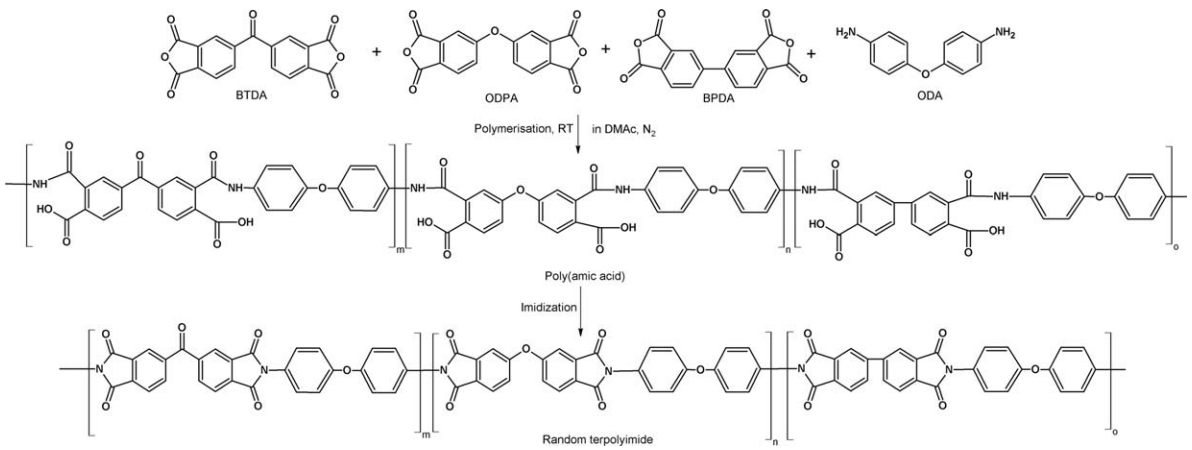

Scheme 2. Synthesis of terpolyimide (TPI).

the degas port. The specific surface area and the pore volume was calculated using Brauner-Emmett-Teller analysis (BET). The particle size of APTS-KIT-6/TPI was measured on a Malvern Zetasizer Nano-S Series using dynamic liquid scattering method. The APTS-KIT-6/TPI composite film specimens of 100 mm long, 5 mm wide, about 0.04 mm thick were cut and the tensile properties were determined following the general procedure in ASTM D882 using 4–5 specimens from each film. The test specimen gauge length was 5 cm and the crosshead speed for film testing was 0.5 cm/min using a Lloyd's instrument with an LF plus model 1 KN load cell. The dielectric properties of the APTS-KIT-6/TPI composite films were measured on a Hioki 3532-50 LCR Hitester at a frequency of 1 MHz. The film sample was plated with a thin silver layer to ensure effective electrical contact and was sandwiched between the electrodes (1 cm diameter). The film samples were heated in a vacuum oven at a temperature of about 120°C for 2 h to remove any condensed moisture present on the film samples. Two specimens from each film sample were taken for measurement to test the reproducibility. The thickness of the film samples for studying tensile properties and dielectric properties was measured with an accuracy of 0.001 mm using co-ordinate measuring machine, TESA microhite 3D (Table I).

RESULTS AND DISCUSSION

Characterisation of KIT-6, calcined KIT-6 and APTS-KIT-6

XRD Patterns of Calcined KIT-6 and APTS-KIT-6. The XRD pattern of calcined KIT-6 in Figure 1 showed its characteristic intense peak at 0.97° (2θ) due to (211), and other peaks at 1.16° and 1.67° (2θ) due to (220) and (332), respectively. The intensity of the peaks of the calcined KIT-6 was higher than that of the APTS-KIT-6. The sharpness of the peaks proved orderly arrangement of mesopores. In addition, the position of the characteristic peak of APTS-KIT-6 was also shifted from 0.97 to 1.14° (2θ). The other peaks were also slightly shifted to higher 2θ. It could happen, only if the APTS functionalization occurred inside the pore in addition to the external surface. It was also confirmed by the BET surface area results as discussed in Section 3.3.

Table I. Thickness and Density of TPI and APTS-KIT-6/TPI Composite Films

Sample	Thickness range (mm)	Density (g cc^{-1})
TPI	0.037–0.039	1.315
APTS-KIT-6(2%)/TPI	0.032–0.035	1.257
APTS-KIT-6(4%)/TPI	0.035–0.038	1.218
APTS-KIT-6(6%)/TPI	0.036–0.039	1.414
APTS-KIT-6(8%)/TPI	0.038–0.042	1.428
APTS-KIT-6(10%)/TPI	0.031–0.035	1.432

Infra-Red Analysis of As-Synthesized KIT-6, Calcined KIT-6, and APTS-KIT-6. The FTIR spectrum of the as-synthesized KIT-6 showed a broad band at 3467 cm^{-1} due to OH stretching vibration of water and defective OH groups (Figure 2). The presence of locked-in template in it was evident by its CH_2 stretching vibration at 2926 cm^{-1}. The bending vibration of water occurred at 1642 cm^{-1}. The CH_2 bending vibration occurred as a shoulder just below 1500 cm^{-1}. The asymmetric Si—O—Si stretching vibration gave an intense broad band at

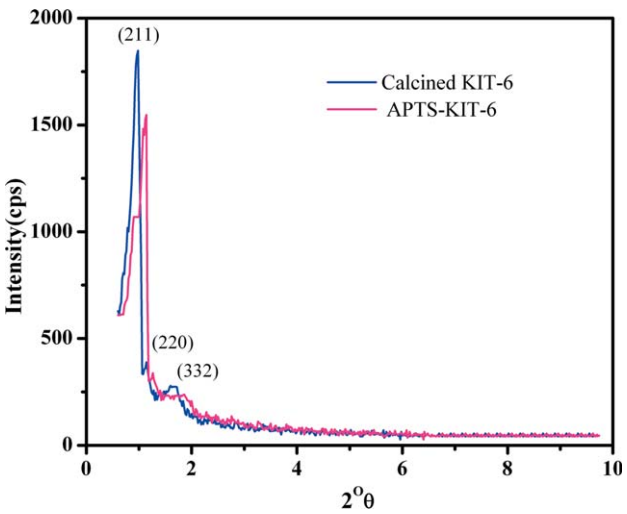

Figure 1. X-Ray diffraction spectra of calcined KIT-6 and APTS-KIT-6. [Color figure can be viewed in the online issue, which is available at wileyonlinelibrary.com.]

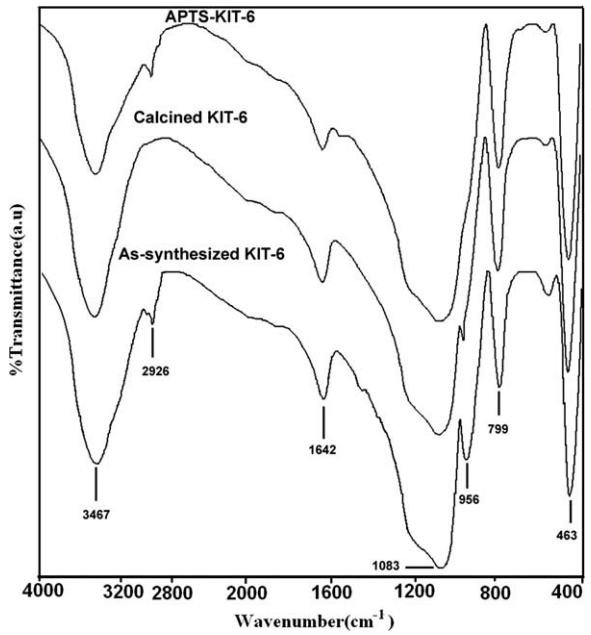

Figure 2. FTIR spectra of as-synthesized KIT-6, calcined KIT-6 and APTS-KIT-6.

1083 cm^{-1}. The defective Si—O—H stretching vibration gave a highly resolved peak at 956 cm^{-1}. The symmetric stretching and bending vibrations of Si—O—Si groups occurred at 799 and 463 cm^{-1}, respectively. The CH_2 stretching and bending vibrations of the template were completely absent in the FTIR spectrum of the calcined KIT-6. The Si—O—H stretching vibration was clearly evident at 970 cm^{-1} even after calcination. Hence the calcined material could be well functionalized with APTS. The CH_2 vibrations of APTS gave a peak close to 2925 cm^{-1} in the FTIR spectrum of APTS-KIT-6. The most compelling evidence for APTS functionalization was arrived by the complete absence of Si—O—H stretching vibration close to 970 $cm^{-1}$and decreased intensity of the peaks due to OH stretching and bending vibrations.[15]

BET Surface Area Analysis and Particle Size Analysis. Characterization of calcined KIT-6 and APTS-KIT-6 by means of BET analysis revealed a significant decrease in the surface area of calcined KIT-6 after APTS functionalization. (Table II). It confirmed anchoring of APTS inside the pores, but anchoring of APTS outside the pores could not be ignored, as the FTIR spectrum of APTS-KIT-6 showed absence of defective Si—O—H groups (Figure 2). The decrease in pore volume of APTS-KIT-6 compared with calcined KIT-6 also confirmed APTS functionalization within the pores. The pore diameter of calcined KIT-6 also showed a significant decrease after APTS functionalization.

Table II. Textural Property of Calcined KIT-6 and APTS-KIT-6

Mesoporous silica	Surface area (m^2 g^{-1})	Average pore diameter (nm)	Pore volume (cm^3 g^{-1})
KIT-6	894	4.79	1.00
APTS-KIT-6	420	2.67	0.44

Table III. Particle Size Distribution of APTS-KIT-6

Size (nm)	Mean intensity (%)
2305	25.4
2669	45.1
3091	28.9
3580	0.5

The particle size range of APTS-KIT-6 was found to be between 2.3 and 3.1 μm (Table III).

Thermogravimetric Analysis

The result of TGA of as-synthesized KIT-6 shown in Figure 3 depicted an initial weight loss below 100°C due to desorption of water. It was followed by a major weight loss at about 350°C due to degradation and desorption of template and the total weight loss was about 21%. The TGA trace of calcined KIT-6 showed a weight loss of 5.3% due to desorption of water. The TGA trace of APTS-KIT-6 showed an initial weight loss of 4.5% due to desorption of water below 100°C, followed by two stages of weight loss due to APTS. It started decomposing close to 300°C and formed a residue, and the latter further decomposed close to 500°C and the total weight loss due to APTS was found to be 5.6%.

Scanning Electron Microscopic Analysis of KIT-6 and APTS-KIT-6

The SEM image of calcined KIT-6 shown in Figure 4(a) was of large irregular-shaped crystals. The terrace of the crystals was not so smooth and the sides revealed piling of plates. The large crystals of parent KIT-6 were reduced to small crystallites in APTS-KIT-6 [Figure 4(b)]. The decrease in size was attributed to sonication applied during functionalization. Such size reduction could admit enhanced APTS functionalization compared with the parent bulk particles.

Characterization of TPI and APTS-KIT-6/TPI Composites

Infra-Red Analysis of TPI and APTS-KIT-6/TPI Composites. In the spectra of TPI depicted in Figure 5, the peaks at 3635 and 3481 cm^{-1} were assigned to OH stretching vibration of free

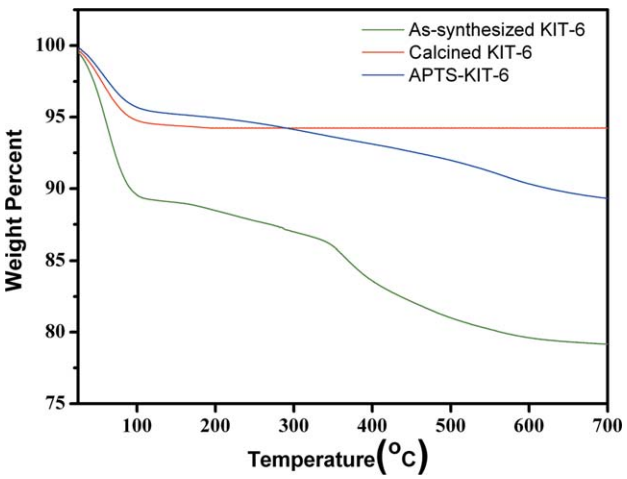

Figure 3. TGA of as-synthesized KIT-6, calcined KIT-6 and APTS-KIT-6. [Color figure can be viewed in the online issue, which is available at wileyonlinelibrary.com.]

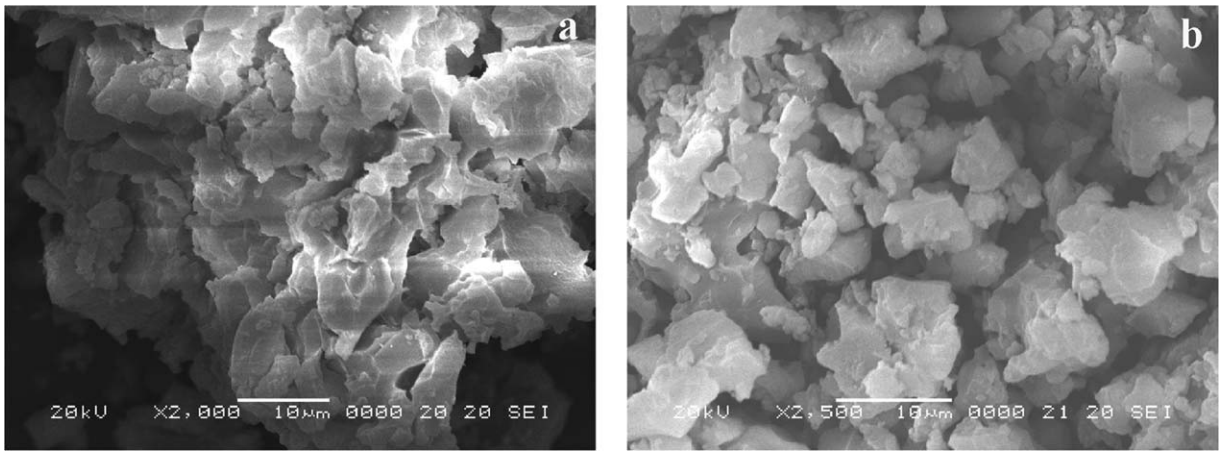

Figure 4. SEM images of (a) calcined KIT-6 (b) APTS-KIT-6.

end COOH group and stretching vibration of asymmetric NH_2 respectively. The asymmetric and symmetric vibrations of imide O═C─N─C═O groups showed their peaks at 1772 and 1713 cm^{-1} respectively, but the peak at 1713 cm^{-1} showed a split due to overlapping symmetric O═C─N─C═O vibration and keto C═O vibration of BTDA. The C─N vibration occurred at 1370 cm^{-1}. The peak at about 1238 cm^{-1} due to phenoxy C─O stretching appeared as a doublet due to ODPA and ODA. Although the spectra of APTS-KIT-6(10%)/TP1 shown in Figure 5 displayed similar features as that of TPI, the presence of mesoporous silica was clearly evident from its Si─O─Si bending vibration occurring close to 450 cm^{-1}.

Thermogravimetric Analysis (TGA). The results of TGA of TPI and APTS-KIT-6/TPI composites illustrated in Figure 6 showed no weight loss below 100°C indicating absence of water/solvent entrapped in the composite matrix. In the TGA trace of TPI, the major weight loss occurred close to 520°C due to its degradation and volatilization. These composites showed single stage decomposition. Hence the imide groups formed by APTS-KIT-6 might also be thoroughly mixed without forming separate domain in the matrix. The degradation resulted in the formation of a carbonaceous residue in all of them. The TGA results of APTS-KIT-6/TPI composites were almost same as that of TPI, but their decomposition temperature was slightly shifted to higher value. The presence of APTS-KIT-6 can develop temperature gradient around the polymer matrix and hence furnace temperature might be slightly different from that of the terpolyimide. Hence, the decomposition temperature of TPI in the composite might have slightly shifted to higher value than that of pure TPI. Lin and Wang[10] also reported an increase in thermal stability for polyimide when APTS-SBA-15 was incorporated.

Differential Scanning Calorimetry. The T_g of TPI illustrated in Figure 7 occurred close to 274°C, but in all the composites it was shifted to slightly higher value. Hence the incorporation of inorganic APTS-KIT-6 might reduce freedom of movement of the polymer chains. In APTS-KIT-6, APTS might be bonded around the entire KIT-6. Hence APTS-KIT-6 is prone to form three dimensional polyimide networks. The polyimide chain could be entirely derived from ODA and/or APTS-KIT-6, hence the imide groups might have high complexity and much randomly oriented. This distribution of polyimide chains restricts

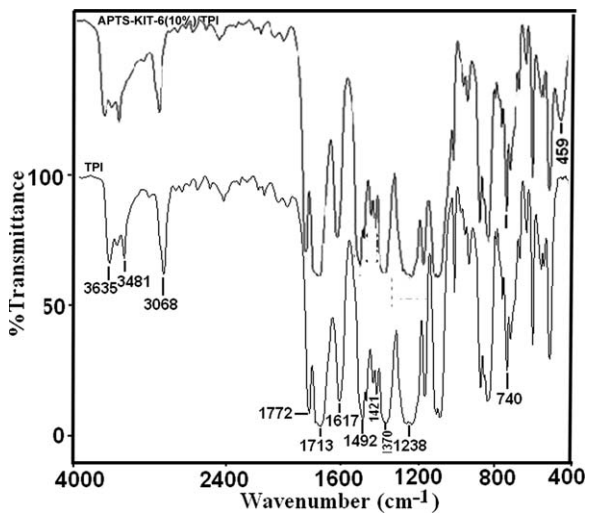

Figure 5. FTIR spectrum of BPDA/BTDA/ODPA-ODA terpolyimide (TPI) and APTS-KIT-6(10%)/TP1.

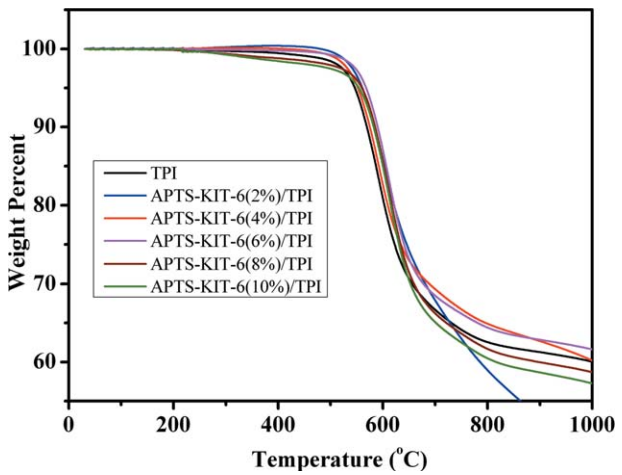

Figure 6. TGA results of TPI and APTS-KIT-6/TPI. [Color figure can be viewed in the online issue, which is available at wileyonlinelibrary.com.]

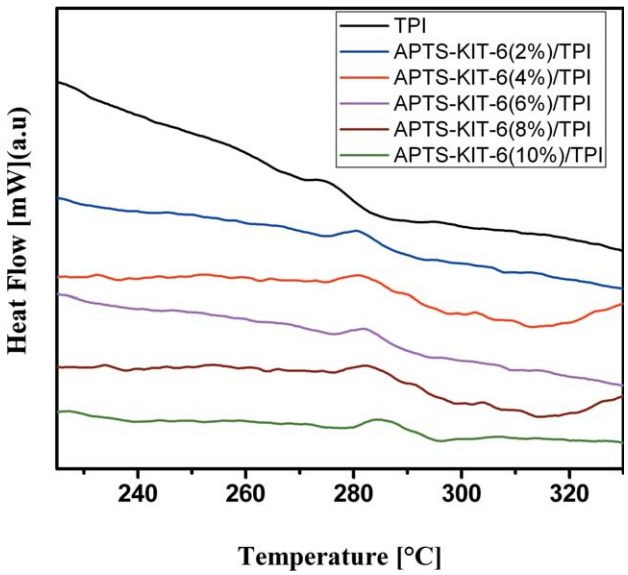

Figure 7. DSC of TPI and APTS-KIT-6/TPI. [Color figure can be viewed in the online issue, which is available at wileyonlinelibrary.com.]

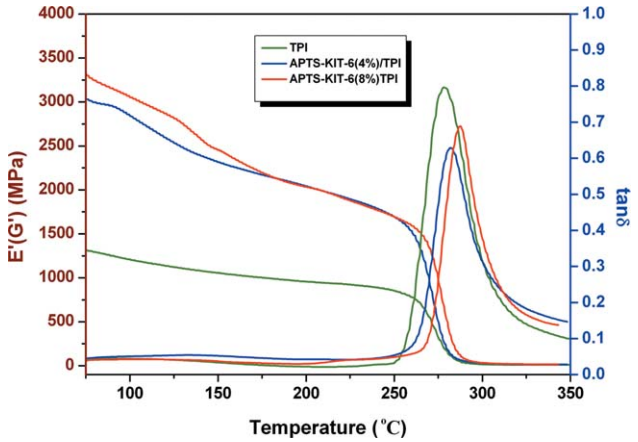

Figure 8. The storage moduli and tanδ of TPI and APTS-KIT-6/TPI as a function of temperature at 1 Hz. [Color figure can be viewed in the online issue, which is available at wileyonlinelibrary.com.]

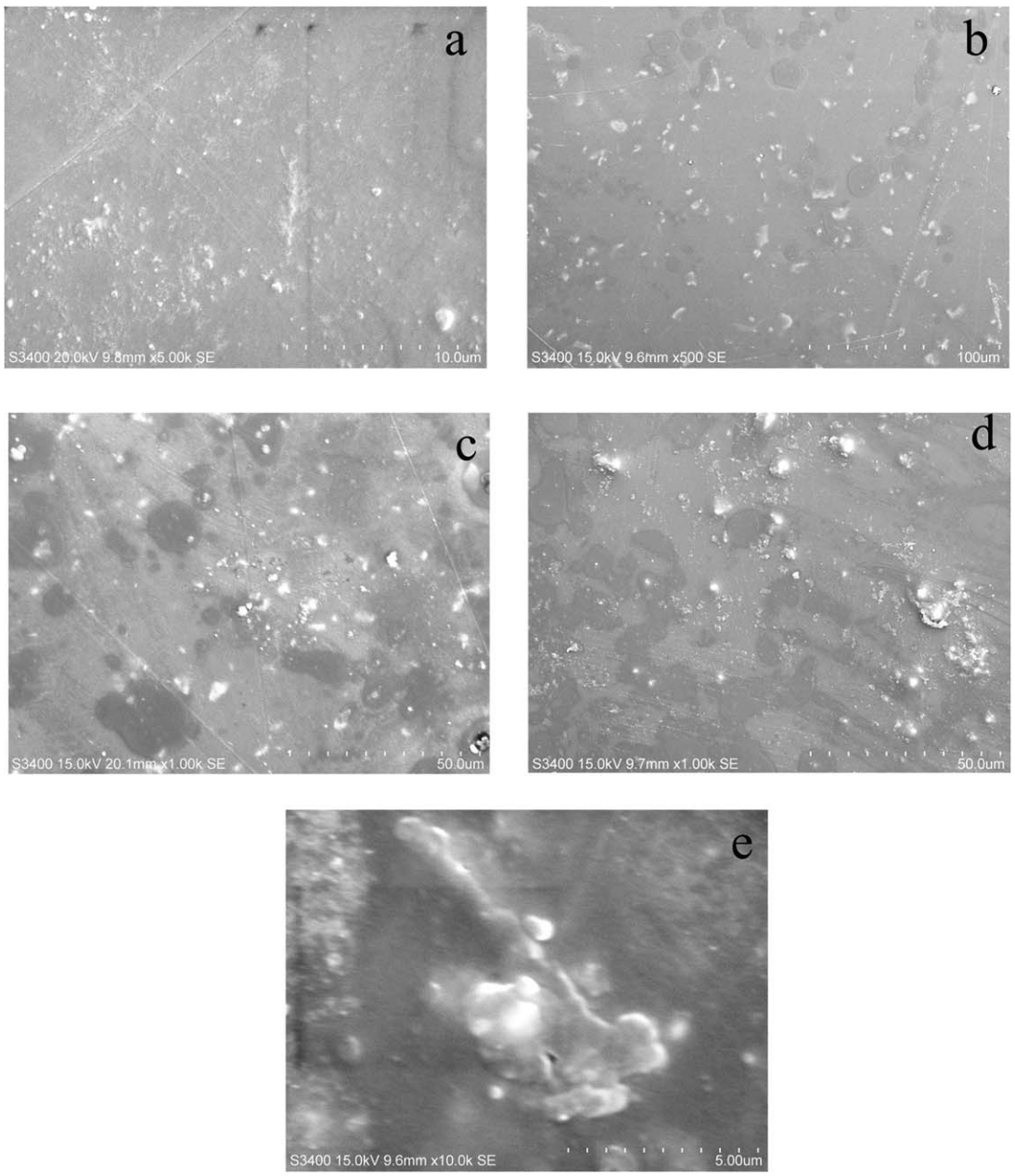

Figure 9. SEM images of APTS-KIT-6/TPI: (a) 2% (b) 4% (c) 6% (d) 8% (e) 10% APTS-KIT-6 loading. [Color figure can be viewed in the online issue, which is available at wileyonlinelibrary.com.]

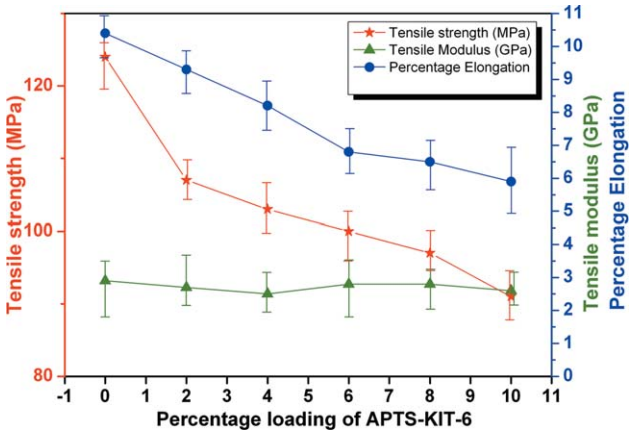

Figure 10. Effect of percentage loading of APTS-KIT-6 on mechanical properties of TPI. [Color figure can be viewed in the online issue, which is available at wileyonlinelibrary.com.]

motion in all the three directions. All of them could contribute to enhance T_g. The complex orientation of polyimide chain is to increase with the increase in the loading of APTS-KIT-6. Therefore the T_g increased with increase in APTS-KIT-6 loading. Even if there is a terpolyimide chain formed entirely with ODA, it cannot make independent contribution to T_g, as it could be entangled and locked by the network formed by APTS-KIT-6. It might be the cause for enhanced T_g of APTS-KIT-6/TPI.

Dynamic Mechanical Properties. TPI showed lower storage modulus than APTS-KIT-6(4%)/TPI and APTS-KIT-6(8%)/TPI (Figure 8). The high storage modulus of composite films was due to formation of cross linked polyimide chains aided by APTS-KIT-6. Such cross linked polyimide chains were to offer high rigidity to the composite film by which the storage modulus increased. The enhancement in storage modulus was also observed from low to high temperatures. Hence such composite films could maintain reliability in applications at elevated temperatures.

The T_g of TPI was slightly lower than APTS-KIT-6/TPI, but the damping intensity (tanδ) of the former was higher than latter. The damping intensity decreased with increase in the APTS-KIT-6 loading. Generally the occurrence of damping is due to polymer chain mobility which produces irreversible heat loss due to friction. The lower the damping value, higher is the rigidity and lower is the intermolecular chain interaction.[17–19] This suggests that the relaxation of the polymer in vicinity of the APTS-KIT-6 surfaces might be lowered around T_g.[20]

Scanning Electron Microscopic Analysis of APTS-KIT-6/TPI Composites. The SEM images of APTS-KIT-6/TPI composites depicted in Figure 9 showed silica particles of unequal size and uneven distribution. Dispersion was very poor at higher loading, due to clustering of particles together [Figure 9(d,e)]. As clustering of particles in the TPI matrix at higher loading can reduce free air volume, it could increase dielectric constant. It was verified in APTS-KIT-6 (8% and 10%)/TPI as discussed in Section 3.12. Therefore higher loading of APTS-KIT-6 above 6% might not be advantageous.

Tensile Properties

The results of tensile strength, tensile moduli and percentage elongation of TPI and APTS-KIT-6/TPI composites are shown in Figure 10. The tensile strength of APTS-KIT-6/TPI composites was lower than that of TPI. It might be due to reduced number of polyimide chains per square centimeter in the composites. It could also reduce the number of polyimide links, as the dimension of APTS-KIT-6 particles is higher than imide repeating units. More importantly, in the imide repeating units there is resonance delocalization of diamine nitrogen lone pair electrons and aromatic ring electrons over the adjacent C═O groups by which the fibers can acquire high tensile strength. In contrast, the delocalization of aromatic ring electrons is absent, when the amino groups of APTS-KIT-6 are converted into imides (Figure 11). The gradual decrease in the tensile strength with the increase in APTS-KIT-6 loading also supported this view. As the amino groups of APTS-KIT-6 might be randomly orientated, the imide fibers might also have random orientations. Hence with the increase in the APTS-KIT-6 loading, the tensile strength decreased. A nonlinear dependence of Young's modulus with increase in loading of KIT-6 was noted. Similar nonlinear variation was reported by Lin and Wang[10] for polyimide/SBA-15. A dramatic decrease in percentage elongation was noted for APTS-KIT-6/TPI compared with TPI. It indirectly established coiling of imide chain in TPI, but coiling might be

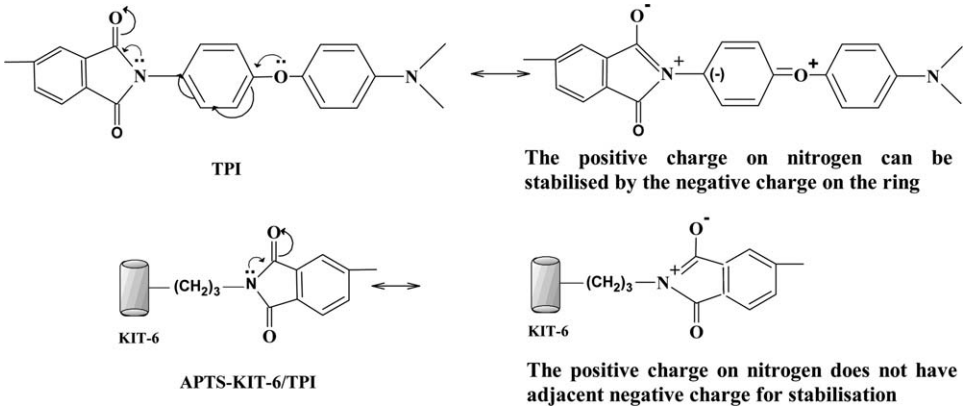

Figure 11. Resonance in TPI and APTS-KIT-6/TPI.

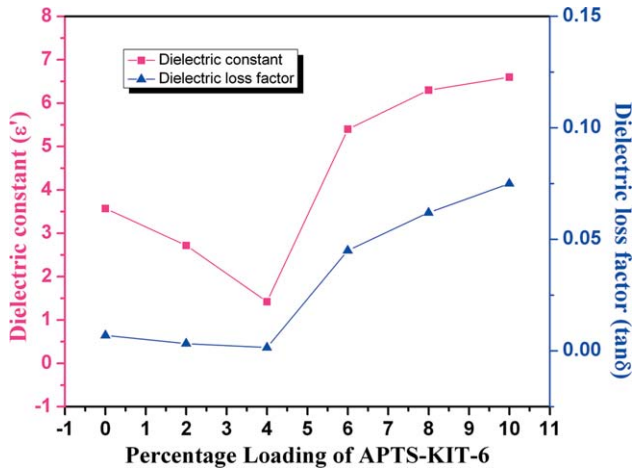

Figure 12. Effect of percentage loading of APTS-KIT-6 on dielectric properties of TPI at 1 MHz. [Color figure can be viewed in the online issue, which is available at wileyonlinelibrary.com.]

suppressed in APTS-KIT-6/TPI composites. In TPI, the imide groups of one repeating unit can have dipole-dipole interaction with the same polymer chain or that of other adjacent polymer chain. But such dipole-dipole interaction might be suppressed in APTS-KIT-6/TPI. Hence TPI showed higher percentage elongation than APTS-KIT-6/TPI composites.

Dielectric Properties

The dielectric constant and dielectric loss factor of TPI and APTS-KIT-6/TPI are shown in Figure 12. The dielectric constant of APTS-KIT 6/TPI decreased with increase in APTS-KIT-6 loading up to 4% and then increased steadily. Low dielectric constant of APTS-KIT-6(4%)/TPI was ascribed to (i) reduction of free Si—OH, (ii) enhancement of hydrophobic property, (iii) large amount of entrapped air in the mesopores and interfacial voids, (iv) uniform dispersion of APTS-KIT-6 and (v) adequate amount of APTS-KIT-6. Low values of the dielectric loss are indicative of minimal conversion of electrical energy into heat in the dielectric material. The low dielectric constant and dielectric loss indicate low electric signal loss in the dielectric medium. The steady increase in dielectric constant with the increase in APTS-KIT-6 loading above 4% was due to poor dispersion, as a result of clustering of particles (Figure 9). Such clustering decreased the interfacial air voids drastically. This is also indicated in the density values (Table I). In addition, the surface morphology of APTS-KIT-6 might also play an important role in increasing the dielectric constant. Since the surface of APTS-KIT-6 particles (Figure 4) was very rough, they could very well associate with polyimide matrix. Such association could further reduce interfacial air voids. Similar reasoning was also reported by Lin and Wang.[10]

CONCLUSIONS

APTS-KIT-6/TPI composite films were prepared by reacting ODA and APTS-KIT-6 with BPDA, BTDA and ODPA via in situ polymerization followed by thermal imidization. APTS-KIT-6(4%)/TPI possessed low dielectric constant (1.42) than all other composites. The reduction in dielectric constant and dielectric loss factor is attributed to the incorporation of air into the mesopores and the interfacial voids (free volume) between the mesoporous silica and polyimide matrix due to introduction of large-sized domains. For higher loadings of APTS-KIT-6 above 4% the dielectric properties increased due to clustering of mesoporous silica. The decomposition temperature of APTS-KIT-6/TPI was slightly higher than the pure TPI. The tensile strength of APTS-KIT-6/TPI composites decreased with the increase in the content of mesoporous silica. The covalent interaction of functionalized KIT-6 and polyimide matrix can minimize the deterioration of mechanical properties. These results indicate that KIT-6 functionalized with APTS can be incorporated into polyimide to reduce dielectric constant, without compromising thermal and mechanical properties. The low dielectric constant and dielectric loss indicate low electric signal loss in the dielectric medium and hence the polyimide composites are suitable for interlayer dielectric applications such as flexible printed circuit boards and other microelectronic applications.

ACKNOWLEDGMENTS

The authors are grateful to B.S.Abdur Rahman University for financial support. The technical support of Mr. Selvam, Anjan Chemicals, for FTIR, Dr.P. Hemalatha and Dr.M. Bhagyalakshmi, for XRD, BET, TGA, and SEM, K. Balachander, Mettler-Toledo for DSC and TGA, Dr. Rajendran and Dr.Ramasamy, CIF, Pondicherry University for SEM, Mr. G. Sakthivel for density and particle size analysis and, Ms. H. Sofia for English correction are greatly appreciated.

REFERENCES

1. Chao, C. C.; Scholz, K. D.; Leibovitz, J.; Cobarruiaz, M.; Chung, C.C. *IEEE T. Compon. Hybr.* **1989**, *12*, 180.
2. Hergenrother, P. M.; Watson, K. A.; Smith, J. G., Jr; Connella, J. W.; Yokota, R. *Polymer* **2004**, *45*, 5441.
3. Kim, M. H.; Lee, K. W. *Met. Mater. Int.* **2006**, *12*, 425.
4. Simpson, J. O.; Clair, A. K. S. *Thin Solid Films* **1997**, 308–309, 480.
5. Maier, G. *Prog. Polym. Sci.* **2001**, *26*, 3.
6. Miyagawa, T.; Fukushima, T.; Oyama, T.; Iijima, T; Tomoi, M. *J. Polym. Sci. A Polym. Chem.* **2003**, *41*, 861.
7. Chen, Y. W.; Wang, W.C.; Yu, W.H.; Kang, E. T.; Neoh, K.G.; Vora, R. H.; Ong, C. K.; Chen, L. F. *J. Mater. Chem.* **2004**, *14*, 1406.
8. Chen, Y. W.; Wang, W. C.; Yu, W. H.; Yuan, Z. L.; Kang, E. T.; Neoh, K. G.; Krauter, B.; Greiner, A. *Adv. Funct. Mater.* **2004**, *14*, 471.
9. Leu, C. M.; Chang, Y. T.; Wei, K. H. *Chem. Mater.* **2003**, *15*, 3721.
10. Lin, J.; Wang, X. *Polymer* **2007**, *48*, 318.
11. Min, C. K.; Wu, T. B.; Yang, W. T.; Chen, C. L. *Compos. Sci. Technol.* **2008**, *68*, 1570.
12. Chung, C. L.; Hsiao, S. H. *Polymer* **2008**, *49*, 2476.

13. Hsiao, S. H.; Guo, W.; Chung, C. L.; Chen, W. T. *Eur. Polym. J.* **2010**, *46*, 1878.
14. Purushothaman, R.; Bilal, I. M.; Palanichamy, M. *J. Polym Res.* **2011**, *18*, 1597.
15. Purushothaman, R. Ph.D Thesis, Anna University, Chennai, India, December **2011**.
16. Won, J. S.; Jung, S. C.; Wha, S. A. *Microporous Mesoporous Mater.* **2008**, *113*, 31.
17. Tsai, M. H.; Whang, W. T. *J. Appl. Polym. Sci.* **2001**, *81*, 2500.
18. Chiang, P. C.; Whang, W. T.; Tsai, M. H. *Thin Solid Films* **2003**, *447*, 359.
19. Tsai, M. H.; Chiang, P. C.; Whang, W. T.; Ko, C. J.; Huang, S. L. *Surf. Coat. Technol.* **2006**, *200*, 3297.
20. Park, C.; Smith, J. G.; Connell, J. W.; Lowther, S. E.; Working, D. C.; Siochi, E. *J. Polymer* **2005**, *46*, 9694.